

# Lawrence Berkeley National Laboratory

## LBL Publications

### Title

X-ray absorption and magnetic circular dichroism studies of Co<sub>2</sub>FeAl in magnetic tunnel junctions

### Permalink

<https://escholarship.org/uc/item/9d44x44t>

### Authors

Ebke, D.  
Kugler, Z.  
Thomas, P.  
et al.

### Publication Date

2010-05-01

# X-ray absorption and magnetic circular dichroism studies of $\text{Co}_2\text{FeAl}$ in magnetic tunnel junctions

Daniel Ebke<sup>1</sup>, Zoë Kugler<sup>1</sup>, Patrick Thomas<sup>1</sup>, Oliver Schebaum<sup>1</sup>, Markus Schäfers<sup>1</sup>, Dennis Nissen<sup>1</sup>, Jan Schmalhorst<sup>1</sup>, Andreas Hütten<sup>1</sup>, Elke Arenholz<sup>2</sup> and Andy Thomas<sup>1</sup>

<sup>1</sup>Thin Films and Physics of Nanostructures, Physics Department, Bielefeld University, Bielefeld 33615, Germany

<sup>2</sup>Advanced Light Source, Lawrence Berkeley National Laboratory, Berkeley, California 94720, USA

**The bulk magnetic moment and the element specific magnetic moment of  $\text{Co}_2\text{FeAl}$  thin films were examined as a function of annealing temperature by alternating gradient magnetometer (AGM) and X-ray absorption spectroscopy (XAS) / X-ray magnetic circular dichroism (XMCD), respectively. A high magnetic moment can be achieved for all annealing temperatures and the predicted bulk and interface magnetic moment of about  $5\mu_B$  are reached via heating. We will also present tunnel magnetoresistance (TMR) values of up to 153% at room temperature and 260% at 13 K for MgO based magnetic tunnel junctions (MTJs) with  $\text{Co}_2\text{FeAl}$  and Co-Fe electrodes.**

*magnetic films, magnetoresistance, thin films, x-ray spectroscopy*

## I. INTRODUCTION

Spintronic devices have found a lot of attention in the recent years due to the possible new applications, e.g. a magnetic random access memory (MRAM) [1,2]. The spin of the electrons is used as an additional degree of freedom in contrast to common electronic devices. Materials with a high spin polarization are eligible for applications. A half metallic behavior, i. e. they are 100% spin polarized at the Fermi level  $E_F$  has been theoretically predicted for some oxide compounds such as  $\text{Fe}_3\text{O}_4$  and  $\text{CrO}_2$  [3], perovskites (e. g.  $\text{LaSrMnO}_3$  [4]), zinc-blende-type CrAs [5] and Heusler compounds [6]. In particular, Co-based Heusler compounds are promising materials for spintronics applications due to the required high Curie temperatures  $T_C$  [7]. A Heusler compound is given by the composition  $X_2YZ$  in the  $L2_1$  structure, where X and Y are transition metal elements and Z is a group III, IV or V element. The main constituent of many spintronic devices is a magnetic tunnel junction (MTJ) with two ferromagnets separated by a thin insulating tunnel barrier [8]. The resistance of such a device depends on the magnetic orientation of the ferromagnets. Usually,  $R_{AP}$  (antiparallel) is higher than  $R_P$  (parallel) and a tunnel magnetoresistance (TMR) can be defined as  $(R_{AP} - R_P)/R_P$ .

Recently, TMR ratios of over 600% at room temperature for a single MgO tunnel barrier [9] and over 1000% for a double MgO barrier were reported [10]. High room temperature TMR ratios have also been reported for magnetic tunnel junctions containing Heusler compounds as electrodes: 217% for  $\text{Co}_2\text{MnSi}$  [11] and very recently 386% for  $\text{Co}_2\text{Fe}_{0.5}\text{Al}_{0.5}\text{Si}$  [12]. Later was grown by using molecular beam epitaxy in place of sputtering deposition. For  $\text{Co}_2\text{FeAl}$  a huge TMR ratio of up to 330% was found very lately, too [13]. The corresponding low temperature TMR ratios are much higher and one challenge is to conserve these values at room temperature, too. This might be realized by shifting the  $E_F$  into the middle of the band gap [12] and is reported to be realized for the compound  $\text{Co}_2\text{Fe}_{0.5}\text{Al}_{0.5}\text{Si}$  which shows a lower temperature dependent TMR ratio compared to  $\text{Co}_2\text{MnSi}$ .

On the other hand, the huge TMR ratio of  $\text{Co}_2\text{FeAl}$  are reported to issue from a extremely flat surface morphology [13].

Here, we present X-ray absorption spectroscopy (XAS) and X-ray magnetic circular dichroism (XMCD) measurements of  $\text{Co}_2\text{FeAl}$  thin films which were performed at beamline 6.3.1 of the Advanced Light Source, Berkeley, USA. The Co- and Fe- $L_{3,2}$  edges were investigated. Surface-sensitive total electron yield TEY was recorded with a grazing angle of incidence of  $30^\circ$  to the sample surface. The XMCD spectra were obtained by applying a magnetic field of  $\pm 2$  T along the x-ray beam direction using elliptically polarized radiation with a polarization of 60%. The XAS intensity and the XMCD effect are defined as  $(I_+ + I_-) / 2$  and  $I_+ - I_-$ , respectively. Here,  $I_+$  and  $I_-$  name the parallel and antiparallel orientation of photon spin to the magnetic field. Furthermore, full MTJs containing a  $\text{Co}_2\text{FeAl}$  electrode were prepared. A high room temperature TMR ratio with a similar low temperature dependence as reported for  $\text{Co}_2\text{Fe}_{0.5}\text{Al}_{0.5}\text{Si}$  can be found [12].

## II. PREPARATION OF TUNNEL JUNCTIONS

DC/RF magnetron sputtering was used for the preparation of our magnetic tunnel junctions. All films were deposited at room temperature. A base pressure of  $1.0 \times 10^{-7}$  mbar of the sputtering system can be achieved; the Argon process pressure is about  $1.5 \times 10^{-3}$  mbar. The layers were deposited on a MgO (001) substrate covered by a 5 nm thick MgO buffer layer to coat surface contaminations. Thereafter, the lower electrode of 20 nm  $\text{Co}_2\text{FeAl}$  was deposited and followed by the MgO tunnel barrier. The lattice mismatch of about 5% of MgO ( $4.21 \times \sqrt{2} = 5.95$  Å [14]) and the  $\text{Co}_2\text{FeAl}$  compound (5.70 Å in our case) rotated by 45 degrees allows for a coherent growth of the layer stack. Afterwards, the counter electrode composed of 5 nm  $\text{Co}_{70}\text{Fe}_{30}$ , 10 nm of  $\text{Mn}_{83}\text{Ir}_{17}$ , 40 nm Ru, and 20 nm Au was deposited. This electrode was omitted for the AGM and XMCD measurements. The layer stacks were ex-situ vacuum annealed at different temperatures to induce crystallization and ordering of the lower layer stack up to the Co-Fe electrode. The samples were cooled in a

magnetic field of 0.65 T to set the exchange bias of the pinned electrode and patterned by optical lithography and ion beam etching to form the tunnel junctions. All transport characterizations were carried out by conventional two terminal measurements.

### III. RESULTS

The transport properties of the MTJs were measured as a function of an external magnetic field for 1.8 nm and 2.1 nm thick MgO barriers. The measurements were done in a temperature range between 13K and room temperature. The applied bias voltage was 10 mV.

#### FIGURE 1 HERE

Fig. 1 depicts an increasing room temperature TMR ratio with increasing annealing temperature. This is also found in conventional Co-Fe-B/MgO/Co-Fe-B MTJs [9] and can probably be attributed to an improvement of the crystallinity of the Heusler/tunnel barrier interface.

Furthermore a good annealing temperature stability can be found for temperatures between 410°C and 470°C. The obtained TMR ratio stays roughly constant in this range. This is in contrast to other studies where the Mn diffusion of the Mn-Ir towards the upper barrier interface was thought to be responsible for the decrease of the TMR ratio beyond 400°C [15]. On the other hand, a similar behavior was reported by Kant et al. and Palusker et al. [16-18].

Fig. 2a shows the temperature dependent TMR ratio for a junction with a 2.1nm thick MgO barrier and annealed for 1h at 450°C. In contrast to the dependency found for Co<sub>2</sub>MnSi [11] junctions ( $\Gamma_{\text{CMS}} = \text{TMR(LT)} / \text{TMR(RT)} = 3.5$ ) it is comparable weak ( $\Gamma_{\text{CFA}} = 1.7$ ) as reported for Co<sub>2</sub>Fe<sub>0.5</sub>Al<sub>0.5</sub>Si [12] and Co<sub>2</sub>FeAl [13] ( $\Gamma_{\text{CFAS}} = \Gamma_{\text{CFA}} = 2.1$ ). Therefore, it has to be reconsidered if the origin of the reported weak temperature dependence is related to a shift of the Fermi level into the gap [12].

#### FIGURE 2 HERE

The corresponding major loops for room temperature and 13 K are shown in Fig. 2b. A TMR ratio of 153% and 260% were achieved, respectively. This is only about half the value reported very recently by Wang et al. [13]. The lowered TMR ratio might be attributed to a higher surface roughness, caused by a different seed layer system. Further investigations of the origin are planned.

The element specific magnetic properties of the Co<sub>2</sub>FeAl/MgO interface were investigated by surface sensitive X-ray absorption spectroscopy (XAS) and X-ray magnetic circular dichroism (XMCD). Both were measured at room temperature in total electron yield with a sampling depth of about 2nm [19, 20].

#### FIGURE 3 HERE (TWO COLUMN)

Fig. 3 shows the Fe- and Co-XAS (Fig. 3a) and XMCD (Fig. 3b) spectra for the as prepared and annealed half

junctions. The measured XAS intensity was normalized to the intensity prior the Fe-L<sub>3</sub> and Co-L<sub>3</sub> edge, respectively.

The arrows indicate prominent features in the XAS. In case of Co the shoulder can be attributed to a certain atomic and magnetic order of the Co<sub>2</sub>FeAl compound at the barrier interface as previously reported for Co<sub>2</sub>MnSi [21, 22]. This feature is already present for the non-annealed sample and is pronounced with increasing annealing temperatures.

By contrast the shoulder in the Fe-XAS of the non-annealed layers is attributed to FeO [22]. The Fe might be oxidized during the sputtering of the MgO barrier. For annealing temperatures higher 200°C no FeO can be found from the XAS. The absent might be explained by the crystallization process of the barrier and the binding of O.

The corresponding Fe- and Co-XMCD in Fig. 3b shows an asymmetry for all annealing temperatures, i.e. a magnetic moment can be achieved even for the non-annealed Heusler layer. This is in contrast to the results for Co<sub>2</sub>MnSi [21] and emphasizes the low ordering temperature of Co<sub>2</sub>FeAl [23].

#### FIGURE 4 HERE

Fig. 4a shows the Fe- and Co-XAS intensity at the L<sub>3</sub> edge (L<sub>3</sub>, as defined in Fig. 3a) as a function of annealing temperature. Above annealing temperature of 200°C the XAS intensity decreases for Co and Fe, respectively. This might be because of an Al segregation below the barrier interface to improve the Heusler structure.

The element specific magnetic moment was calculated from the XMCD by applying the sum rules [24]. A number of 3d holes  $n_d=1.93$  for Co and  $n_d=3.29$  for Fe were assumed. This was carried out from SPR-KKR density of band calculation [25]. As shown in Fig. 4b the magnetic moment of the Co atoms measure up to the predict value of 1.14  $\mu_B$  for the full range of annealing temperature. The reference values are represented by the dashed lines. In contrast the Fe magnetic moment is increased with increasing annealing temperatures and is close to the predicted value of 2.81  $\mu_B$  for the 500°C annealed sample [26]. This might be because of the reduction of FeO. A similar behavior is found for the total moment resulting from  $2 \times m_{\text{Co}} + m_{\text{Fe}}$ . The predicted bulk value of 4.99  $\mu_B$  can be reached for annealing temperatures higher 400°C [26].

This is also found for the bulk moment of the Co<sub>2</sub>FeAl layers that was investigated by an alternating gradient field magnetometer (AGM) at room temperature. Here, the reported bulk value of 4.99  $\mu_B$  (1007 kA/m and assuming L<sub>21</sub> structure with a experimental lattice constant of 5.69 Å) is reached independently of annealing temperature.

### IV. CONCLUSION

We have investigated the magnetic and electronic transport properties of the Heusler compound Co<sub>2</sub>FeAl. A low temperature TMR ratio of up to 260% was achieved. Due to a weak temperature dependence this results in up to 153% at room temperature. The comparatively low values might be attributed to a higher surface roughness of the Heusler layer, due to a different seed layer system that was used in this work.

A high bulk and interface magnetic moment of the Heusler layer are present in the as prepared state. The predicted values for the bulk moment as well as for the element specific interface moment can be reached via annealing.

#### ACKNOWLEDGMENT

This work was financially supported by the German Bundesministerium für Bildung und Forschung (BMBF) for within the project HeuSpin. The authors gratefully acknowledge the support of the Advanced Light Source at Berkeley. The Advanced Light Source, Berkeley, USA, is supported by the Director, Office of Science, Office of Basic Energy Sciences, of the U.S. Department of Energy under Contract No. DE-AC02-05CH11231. We thank A. Weddemann for band structure calculations.

#### REFERENCES

- [1] S. A. Wolf, D. D. Awschalom, R. A. Buhrman, J. M. Daughton, S. von Molnar, M. L. Roukes, A. Y. Chtchelka-nova, and D. M. Treger, *Science* 294(5546), 1488–1495 (2001)
- [2] G. A. Prinz, *Science* 282(5394), 1660–1663 (1998)
- [3] J. M. D. Coey and M. Venkatesan, *J. Appl. Phys.* 91 8345 (2002)
- [4] W. E. Picket and D. J. Singh, *J. Magn. Magn. Mater.* 172 237 (1997)
- [5] H. Akinaga, T. Manago and M. Shirai. *Jpn. J. Appl. Phys.* 39 p. L1118 (2000)
- [6] R. A. de Groot, F. M. Mueller, P. G. van Engen, and K. H. J. Buschow, *Phys. Rev. Lett.* 50 2024 (1983)
- [7] P. J. Webster, *J. Phys. Chem. Solids* 32 (1971)
- [8] J. S. Moodera and G. Mathon, *J. Magn. Magn. Mater.* **200**, 248 1999
- [9] S. Ikeda, J. Hayakawa, Y. Ashizawa, Y. M. Lee, K. Miura, H. Hasegawa, M. Tsunoda, F. Matsukura and H. Ohno, *Appl. Phys. Lett.* 93 082508 (2008)
- [10] L. Jiang, H. Naganuma, M. Oogane and Y. Ando, *Appl. Phys. Express*, 2 083002 (2009)
- [11] S. Tsunegi, Y. Sakuraba, M. Oogane, K. Takanashi and Y. Ando, *Appl. Phys. Lett.* 93 112506 (2008)
- [12] N. Tezuka, N. Ikeda, F. Mitsuhashi and S. Sugimoto, *Appl. Phys. Lett.* 95 162504 (2009)
- [13] W. Wang, H. Sukegawa, R. Shan, S. Mitani and K. Inomata, *Appl. Phys. Lett.* 95 182502 (2009)
- [14] *Moscow University Geology Bulletin* 47 80 (1992)
- [15] J. Hayakawa, S. Ikeda, Y. M. Lee, F. Matsukura and H. Ohno, *Appl. Phys. Lett.* 89 232510 (2006)
- [16] P. V. Paluskar, C. H. Kant, J. T. Kohlhepp, A. T. Filip, H. J. M. Swagten, B. Koopmans and W. J. M. de Jonge, 49th Annual Conference on Magnetism and Magnetic Materials, AIP 97 10C925 (2005)
- [17] C. H. Kant, J. T. Kohlhepp, H. J. M. Swagten and W. J. M. de Jonge, *Appl. Phys. Lett.* 84 1141-1143 (2004)
- [18] C.H. Kant, J.T. Kohlhepp, P.V. Paluskar, H.J.M. Swagten and W.J.M. de Jonge, *J. Magn. Magn. Mater.* 286 154-157 (2005)
- [19] R. Nakajima, J. Stöhr and Y. U. Idzerda, *Phys. Rev. B* 59(9), 6421 (1999)
- [20] Y. U. Idzerda, C. T. Chen, H. J. Lin, G. Meigs, G. H. Ho and C. C. Kao, *Nucl. Instrum. Methods Phys. Res. A* 347(1-3), 134-141 (1994)

- [21] J. Schmalhorst, S. Kämmerer, M. Sacher, G. Reiss and A. Hütten, *Phys. Rev. B* 70(2) 024426 (2004)
- [22] W. Regan, *Phys. Rev. B*, 64(21) 214422 (2001)
- [23] D. Ebke, P. Thomas, O. Schebaum, M. Schäfers, D. Nissen, A. Hütten and A. Thomas, *J. Magn. Magn. Mater.*, *accepted* (2009)
- [24] Chen, C. T., Idzerda, Y. U., Lin, H.-J., Smith, N. V., Meigs, G., Chaban, E., Ho, G. H., Pellegrin, E., and Sette, F. *Phys. Rev. Lett.* 75(1), 152–July (1995)
- [25] H. Ebert, the Munich SPR-KKR package, Version 3.6, <http://olymp.cup.uni-muenchen.de/ak/ebert/SPRKKR>; H. Ebert, in *Electronic Structure and Physical Properties of Solids*, Lecture Notes in Physics Vol. 535, edited by H. Dreyssè Springer, Berlin, 2000, p. 191
- [26] I. Galanakis, *Phys. Rev. B* 71(1) 012413 (2005)

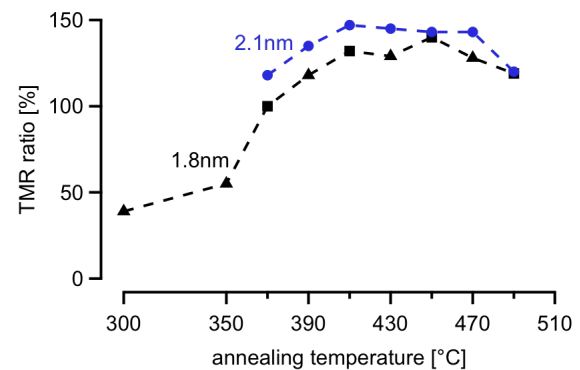


Fig. 1: Room temperature TMR ratios for  $\text{Co}_2\text{FeAl/MgO/Co-Fe}$  junctions at different annealing temperatures. The squares and triangles indicate the two different subsequently annealed samples for the 1.8 nm thick MgO barrier.

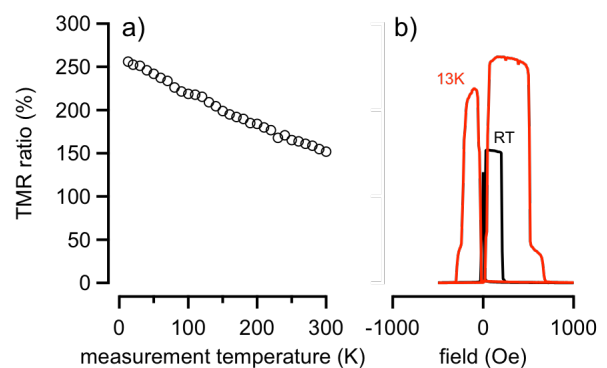


Fig. 2: Temperature dependent TMR ratio for  $\text{Co}_2\text{FeAl/MgO/Co-Fe}$  junctions (a) and the corresponding major loops for RT and 13K (b).

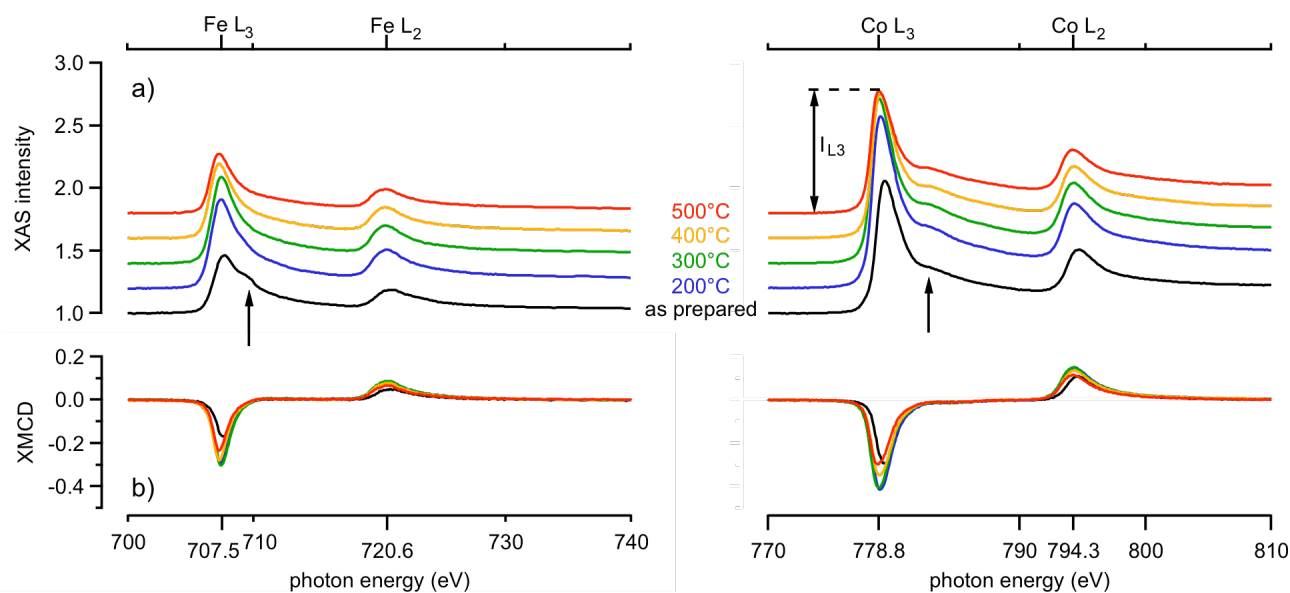


Fig 3: Room temperature XAS (a) and XMCD (b) spectra at the Fe- $L_{3,2}$  and Co- $L_{3,2}$  edge, respectively for different annealing temperatures. The XAS intensities are normalized to the values prior the  $L_3$  edge. For comparison the baseline of the measurement is shifted in regard to the annealing temperature. The arrows mark prominent XAS features.

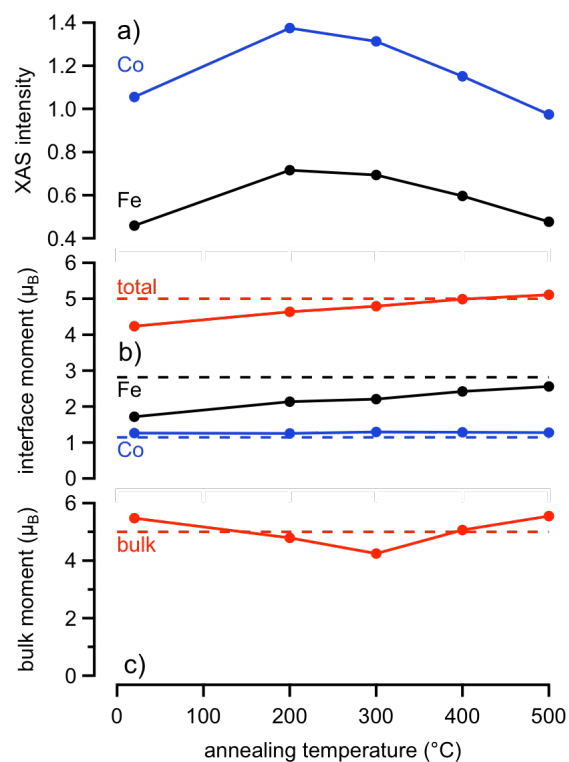


Fig. 4: Room temperature XAS(a), XMCD(b) and AGM (c) investigations of MgO/Co<sub>2</sub>FeAl/MgO layers as a function of annealing temperature. a) XAS intensity at the  $L_3$  edge of Co and Fe, respectively. b) element specific moment (orbital + spin) of the barrier interface and the corresponding total moment ( $2 \times m_{\text{Co}} + m_{\text{Fe}}$ ). c) bulk moment of the Co<sub>2</sub>FeAl layer.